applied sciences

MDPI

Article

In Situ vs. Ex Situ Indentation for Adhesion Evaluation of Nitride/Polymer Interfaces: A Comparative Study Under Controlled Ambient Conditions

Filippo Sabatini [1,*], Emanuele Cattarinuzzi [2], Vincent Coutellier [3], Simone Mariani [2], Davide Fagiani [2], Laurent-Luc Chapelon [3], Andrea Li Bassi [1] and Paola Zuliani [2]

[1] Department of Energy, Politecnico di Milano, via Lambruschini, 20156 Milan, Italy; andrea.libassi@polimi.it
[2] STMicroelectronics Agrate, Camillo Olivetti 2, 20864 Agrate Brianza, Italy; emanuele.cattarinuzzi@st.com (E.C.); simone.mariani@st.com (S.M.); davide.fagiani@st.com (D.F.); paola.zuliani@st.com (P.Z.)
[3] STMicroelectronics Crolles, imm Belledonne 1, 850 r Jean Monnet, 38920 Crolles, France; vincent.coutellier@st.com (V.C.)
* Correspondence: filippo.sabatini@polimi.it

Abstract

This work investigates the reciprocal adhesion of Polybenzoxazole (PBO) and silicon nitride (SiN) with a focus on the combined effects of surface chemistry and environmental conditions, i.e., temperature (T) and relative humidity (RH). A set of six samples, including standard and silicon-rich SiN substrates treated with oxygen (O_2) or carbon tetrafluoride (CF_4) plasma, was fabricated and characterized by AFM, XPS, and TEM/EDX to quantify surface roughness and interfacial chemical modifications. Adhesion with PBO was then assessed through nanoindentation both in situ, during ambient control, and ex situ, after aging in a climatic chamber. Compared to PBO adhesion with as-deposited standard and silicon-rich SiN, O_2 plasma treatment was shown to improve adhesion by 13% and 24%, respectively, whereas CF_4 plasma treatment was still beneficial but more limited, improving adhesion by 8% for both substrates. The different effects were ascribed to the formation of a surface oxide layer after O_2 plasma, enhancing chemical affinity and substantially equalizing the adhesion on the two SiN substrates, while CF_4 plasma was impacting adhesion by reducing the substrates' activity and, thus, increasing the efficiency of the PBO curing procedure. Notably, the adhesion loss with increasing dew point of the ambient (dependent on temperature and relative humidity) was observed across all samples regardless of surface treatment, reinforcing the critical role of absorbed moisture on polymeric film adhesion. However, this trend was observed for all samples only for in situ testing, with a loss of 25% in the critical load of delamination for the most critical environment, while ex situ tests showed a marked recovery of adhesion properties, leading to measurements no longer reflecting the actual state of the samples inside the altered environment. The results presented in this paper highlight the effect of substrate preparation on the adhesion of an organic compound and a substantial difference in environmental control methods for adhesion testing, providing an alternative approach to classical aging treatments and subsequent characterization for qualifying polymer/inorganic interfaces exposed to stressful operational conditions.

Keywords: adhesion; delamination; interface; surface treatment; indentation; dew point; organic compound

Academic Editor: Giacomo Dacarro

Received: 28 January 2026
Revised: 23 February 2026
Accepted: 27 February 2026
Published: 4 March 2026

1. Introduction

Polymeric materials used as protective layers play a crucial role in the manufacturing of advanced microelectronic components, particularly in providing mechanical protection and electrical insulation for devices. Among these materials, polybenzoxazoles (PBO) and polyimides (PI) represent two of the most widely used classes due to their excellent thermal, mechanical, and chemical properties, which are essential for the reliability and operational lifetime of electronic devices. In particular, PBO stands out for its high thermal stability, low dielectric constant, and excellent chemical resistance, making it ideal for high-performance applications in devices subjected to strong thermal cycling and humid environments [1,2]. However, despite these properties, long-term reliability strongly depends on the quality of adhesion between the polymeric film and the underlying inorganic substrate, typically a passivation layer like silicon nitride (SiN), which is nowadays one of the most used materials for this role in the semiconductor industry [3,4].

Recent studies have emphasized that the intrinsic structure and the presence of defects in polymer films can significantly reduce their mechanical properties and adhesive strength [5]. However, it is well known that the main causes of degradation at the interface between polymeric and inorganic substrates are primarily environmental factors such as temperature and humidity [6–9]. These factors can induce internal stresses, delamination, and structural degradation phenomena, which compromise the functionality of the electronic component. Moisture absorption induces significant hygroscopic swelling in polymer films, generating internal stress and promoting the progressive deterioration of adhesion [10–14].

Careful control of the substrate surface preparation can be an effective strategy to maximize adhesive performance and device reliability. Several studies have shown that the surface properties of the substrate, such as roughness, surface chemistry, and preconditioning treatments, can significantly affect adhesion quality [15–18]. The impact of roughness is still not entirely clear, with some studies in the literature indicating an increase in adhesion with increasing roughness due to higher effective contact and mechanical interlocking [19,20], and others showing experimental results of increasing adhesion for smoother substrates [21]. On the contrary, the impact of the substrate surface chemistry, including the presence of oxygenated or fluorinated functional groups, has been shown repeatedly to strongly influence chemical affinity and the formation of interfacial bonds [22–24]. For instance, oxygen plasma treatments are widely used to improve interface adhesion [25–27].

Another significant aspect concerns the possibility of performing adhesion characterizations on samples of interest while controlling the environment or following environmental aging treatments. In the former case, the characterization is in situ, often limited to short retention times in the modified ambient, whereas in the latter, the characterization is ex situ, which permits investigation of aspects related to longer retention times at the cost of performing the adhesion test in a different environment.

The present study aims to characterize through nanoindentation the adhesion of a SiN/PBO interface by varying the SiN substrates stoichiometry, their surface properties through plasma treatments, and the environmental conditions, through the implementation of complementary in situ and ex situ analysis. This approach allowed a better understanding of the differences between the two environmental control methodologies across a diverse set of samples, introducing a valid alternative method to the well-established aging technique to assess interface quality and resistance.

2. Experimental Methods

The experimental set consists of six samples composed of different variants of silicon nitrides as substrate on which identical ~9 μm thick PBO polymer film is deposited via electrospinning and subsequently cured at 350 °C for 60 min under N_2 environment. The SiN substrates were deposited by Plasma Enhanced Chemical Vapor Deposition (PECVD) with a nominal thickness of 0.6 μm on planar silicon wafers (775 μm). To investigate the effect of substrate stoichiometry on adhesion, the chemical composition of SiN was modified by varying the ratio of silane (SiH_4) and ammonia (NH_3) precursors during the deposition process. Two main groups of samples were produced, each consisting of three variants in terms of post-deposition surface treatment. The first group includes standard (St), near-stoichiometric SiN substrates with a nominal Si/N ratio of 0.80, while the second group consists of silicon-rich (SR) SiN substrates with a nominal Si/N ratio of 1.05. Each group includes a sample as-deposited (no surface treatment), a sample treated with oxygen plasma (O_2), and one treated with carbon tetrafluoride plasma (CF_4). Both plasma treatments were applied by inductively coupled plasma (ICP) with an Ultima HDP-CVD Centura reactor (Applied Materials, Santa Clara, CA, USA) with an exposure time of 10 min. All the SiN substrates are described in Table 1.

Table 1. List of SiN substrates analyzed in this study. All samples are composed of a bulk silicon support, a SiN substrate of 0.6 μm thickness and varying stoichiometry, and an upperlying 9 μm PBO film.

Tag	Si/N	Treatment
St_Asd	0.8	As-deposited
St_CF4	0.8	Plasma CF_4
St_O2	0.8	Plasma O_2
SR_Asd	1.05	As-deposited
SR_CF4	1.05	Plasma CF_4
SR_O2	1.05	Plasma O_2

Before PBO deposition, the six substrates were characterized using several analytical techniques; this approach enabled a systematic evaluation of how different surface treatment conditions influence the quality of PBO adhesion on the inorganic substrate. Surface roughness was measured by Atomic Force Microscopy (AFM) using a Bruker Dimension IconXR (Bruker, Billerica, MA, USA), while surface and cross-sectional chemical composition were analyzed by X-ray Photoelectron Spectroscopy (XPS) using a PHI5000 Versaprobe III coupled with argon sputtering for depth profiling (ULVAC-PHI, Chigasaki, KA, Japan) and by Transmission Electron Microscopy (TEM) coupled with Energy Dispersive X-ray Spectroscopy (EDX), using a Themis Z aberration-corrected Scanning Transmission Electron Microscope (Thermo Fisher Scientific, Waltham, MA, USA).

After PBO deposition, it has been possible to evaluate the adhesion on the different substrates and as a function of the external environment, both in situ and ex situ. Due to high baseline adhesion values, standard techniques such as peel tests [28] and four-point bending did not yield adequate results. Thus, adhesion analyses have been performed through nanoindentation using a Bruker TI980 tribo-indenter (Bruker, Billerica, MA, USA) equipped with a high load transducer and a sphero-conical tip with a 20 μm curvature radius. Nanoindentation also offers the advantage of integration with environmental control modules, allowing for in situ analyses directly within the experimental setup. The PBO adhesion to the six analyzed substrates was then evaluated by comparing the critical load for delamination (details in Section 4). One SiN/PBO sample for each substrate and environmental condition has been tested in situ and ex situ (two different sets of samples), and the reported critical load for delamination was obtained by normalizing to

the maximum applied load, using the average curves from six consecutive indentations for each sample.

In situ analyses were performed using the "xSol-Humidity" module, a sample holder designed for specimens with small dimension (~15 × 15 mm), whose internal atmosphere can be controlled by heaters and water vapor injection, controlled respectively by a temperature controller (Model 336, Lake Shore Cryotronics Inc., Westerville, OH, USA) and a humidity generator (HGC30, DataPhysics Instruments GmbH, Filderstadt, BW, Germany) [29]. The feedback to the heaters and the humidity generator is provided by a thermocouple measuring the temperature and a sensor measuring the relative humidity, placed a few millimeters from the sample. A small opening (~4 mm diameter) on the top of the sample holder enables access of the nanoindentation tip to the sample surface. For this purpose, dedicated tips are used, designed with a shaft long enough to cover the full distance between the sample surface and the outer surface of the sample holder. Thus, in situ analysis enables more accurate characterization of adhesive properties, providing data that directly reflect the real operating conditions to which the materials are exposed. The samples were tested in different environments upon reaching the equilibrium condition inside the xSol-Humidity, up to 75 °C and 75% RH, corresponding to the technical limits of the module. The transient time to stabilize the testing condition has always ranged from 30 to 60 min, varying among the different environments.

For ex situ tests, samples were subjected to aging treatments in a climatic chamber for periods of 2 and 7 days. Environmental conditions were varied within maximum limits of 85 °C and 85% RH, corresponding to the operational limits of the climatic chamber used. At the end of each aging period, samples were removed from the climatic chamber and immediately tested via nanoindentation under ambient conditions.

Figure 1 shows all the environmental conditions evaluated in this study for both in situ and ex situ analyses. In addition to temperature and relative humidity values, the figure also includes constant dew point curves, which allow for a univocal identification of the environmental criticality of each condition, and technical tool limits in T and RH.

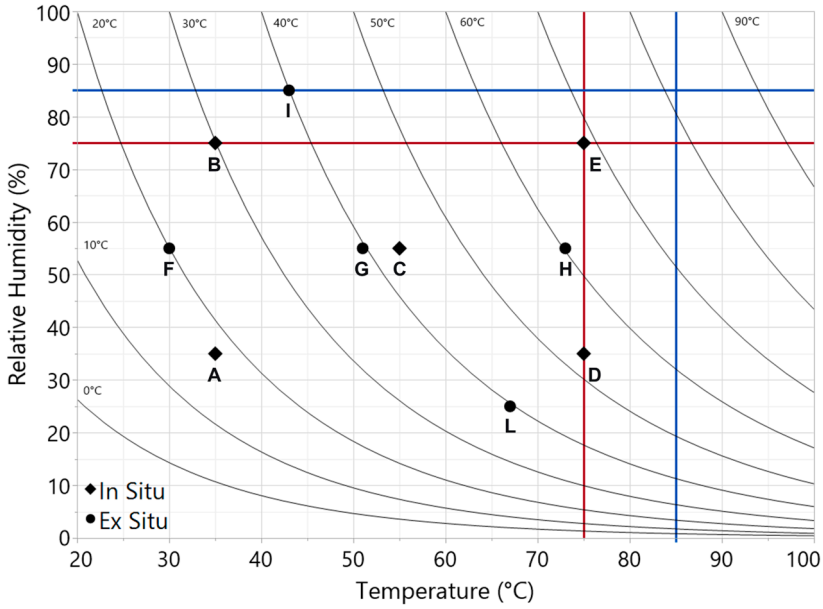

Figure 1. T–RH plot showing the lines of constant dew point (value reported along the plot edge) and the points characterized in this study by the climatic chamber or xSol-Humidity module. The red and blue lines indicate the operational limit of the xSol-Humidity module and the climatic chamber, respectively. The letters present within the figure are related to Table 2 reported below.

Table 2. List of all the ambient conditions tested, indicated by the pair T–RH or univocally by the corresponding T_{DP}, evaluated by the Magnus–Tetens formula (Equation (1)). Each point is tagged with a letter for quicker relocation in Figure 1.

Tag	T (°C)	RH (%)	T_{DP} (°C)	Tool	Analysis
A	35	35	17	xSol | Humid	In Situ
B	35	75	30	xSol | Humid	In Situ
C	55	55	43	xSol | Humid	In Situ
D	75	35	53	xSol | Humid	In Situ
E	75	75	69	xSol | Humid	In Situ
F	30	55	20	Climatic Chamber	Ex Situ
G	51	55	40	Climatic Chamber	Ex Situ
H	73	55	60	Climatic Chamber	Ex Situ
I	43	85	40	Climatic Chamber	Ex Situ
L	67	25	40	Climatic Chamber	Ex Situ

To conclude, Table 2 summarizes all information related to each tested point referenced in Figure 1.

3. Substrates Characterization

The first results concern the characterization of the SiN substrates, performed to obtain information that could help understand and interpret the results related to the adhesion of PBO on the different samples analyzed. To this end, analyses were conducted to determine the morphological and chemical surface properties of the SiN substrates before the deposition of the polymeric film.

AFM analysis permitted the investigation of the surface roughness through the root mean square roughness (Rq) value. Reference results for as-deposited samples are reported in Figure 2, while all results are summarized in Table 3. Analysis reveals relatively flat surfaces but significantly higher roughness for Si-rich nitride substrates, by more than 40% compared to standard nitride ones. A distinct difference is noted in the impact of plasma treatments: while CF_4 plasma does not affect the roughness of the substrates, O_2 plasma effectively reduces this value by approximately 14% across both standard and Si-rich substrates.

XPS analysis confirms nominal stoichiometry for the standard nitride (At% Si/N = 0.8) and shows a small error for the silicon-rich nitride (At% Si/N = 1.08 instead of 1.1). Moreover, the analysis has been coupled with argon sputtering to observe the evolution of several elements in the depth profile of the substrates, reported in Figure 3.

The analysis results for the St_Asd substrate are shown in Figure 3a as a reference for all other substrates investigated. Aside from the obvious presence of silicon and nitrogen, the analysis reports a small quantity of carbon near the interface, most probably related to atmospheric contaminants, and varying amounts of oxygen depending on the surface treatments adopted for the various samples, as reported in Figure 3b. Specifically, the carbon content at the surface (sputtering time equal to zero) remained between 20% and 40% for all samples, rapidly decreasing to near zero at short thicknesses. It is also worth noting that plasma treatments with O_2 result in a higher oxygen content in the samples analyzed, with an average increase measured at the surface (sputtering time equal to zero) of 54% for the St_O2 sample and 74% for the SR_O2 sample, compared to the other four samples. Furthermore, the treatment also led to a much greater oxygen presence in depth compared to samples treated with CF_4 plasma or without any treatment, suggesting a more structured surface variation that will be further discussed with TEM/EDX results. The presence of fluorine was investigated in all samples, but was never found to exceed 2 At%, even in the CF_4 plasma-treated samples, and was therefore considered irrelevant

for adhesion to PBO. Lastly, it was observed that both plasma treatments led to a reduction in carbon content, most likely due to a "cleaning" effect, with a relative reduction in atomic carbon content evaluated at the interface of ~50% for the two O_2-treated samples and ~52% for the two CF_4-treated samples.

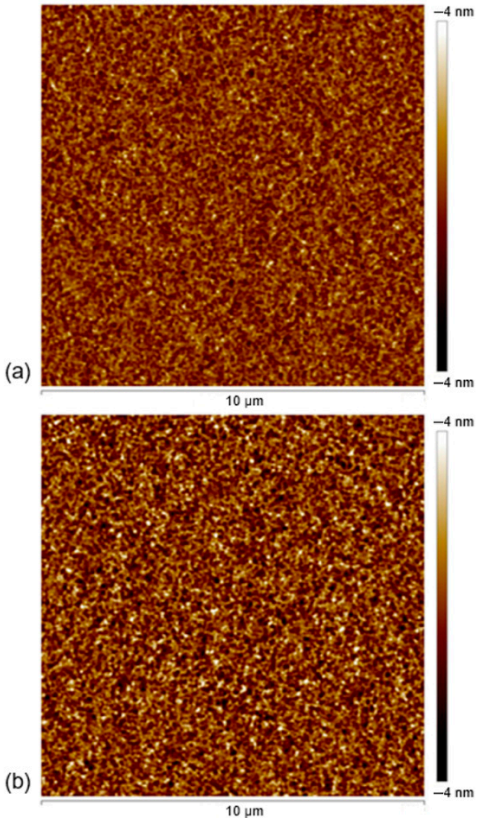

Figure 2. Front view of the standard (**a**) and silicon-rich (**b**) SiN as-deposited substrates analyzed by AFM.

Table 3. AFM analysis results of each substrate by the values of root mean square roughness (R_q) and maximum peak-valley depth (R_{max}) reported in micrometers.

Sample	R_q [µm]	R_{Max} [µm]
St_Asd	0.77	7.18
SR_Asd	1.12	10.1
St_CF4	0.78	7.88
SR_CF_4	1.12	11.0
St_O2	0.66	6.84
SR_O2	0.97	8.63

The effects of plasma treatments on the surface chemical composition of the substrates were further investigated through TEM/EDX analyses. Results are reported in Figure 4 for the St_O2 substrate used as a reference. Again, the impact of oxygen plasma treatment proved to be much more effective, resulting in a significant increase in oxygen concentration at the surface region. Further insights through TEM observation revealed that this increase in oxygen concentration corresponds to the formation of a surface oxidized layer, whose thickness has been optically estimated at around 10 nm for both silicon-rich and standard SiN substrates (see Figure 4b). Results from CF_4 plasma have also shown oxygen presence on the surface, but with lower intensity, of about 20% of atomic presence, reaching half the at% resulting from oxygen plasma. Indeed, the substrate treated with CF_4 plasma shows no presence of a compact oxidized film in the TEM images. Lastly, fluorine signals were

again detected, but only for substrates treated with CF_4 plasma and always for low atomic percentages, thus its impact has been considered non- influential for adhesion properties.

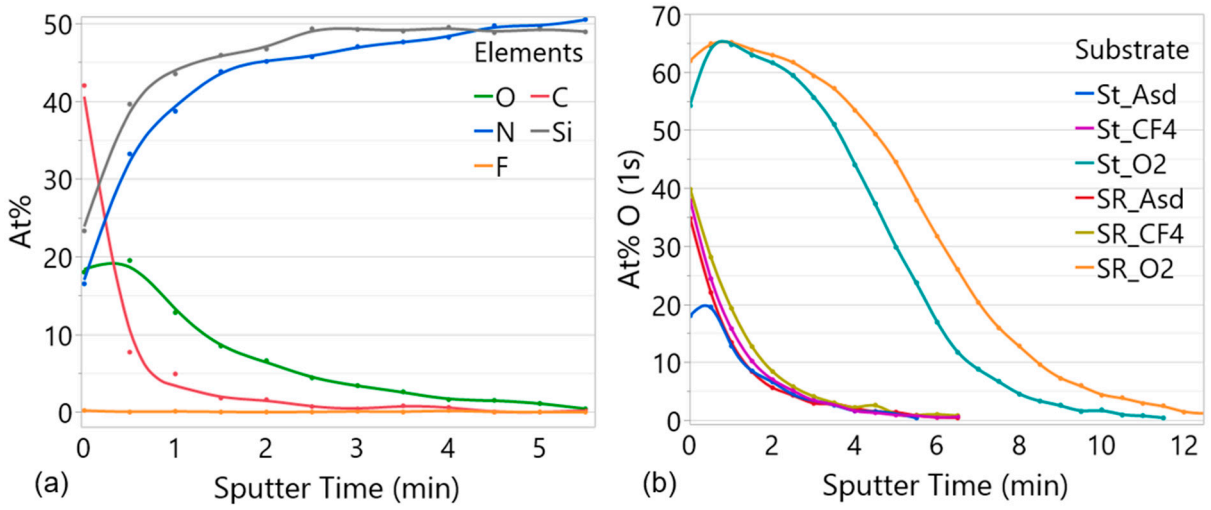

Figure 3. XPS analysis reported for the St_Asd substrate used as reference (**a**), and for oxygen content in all substrates (**b**).

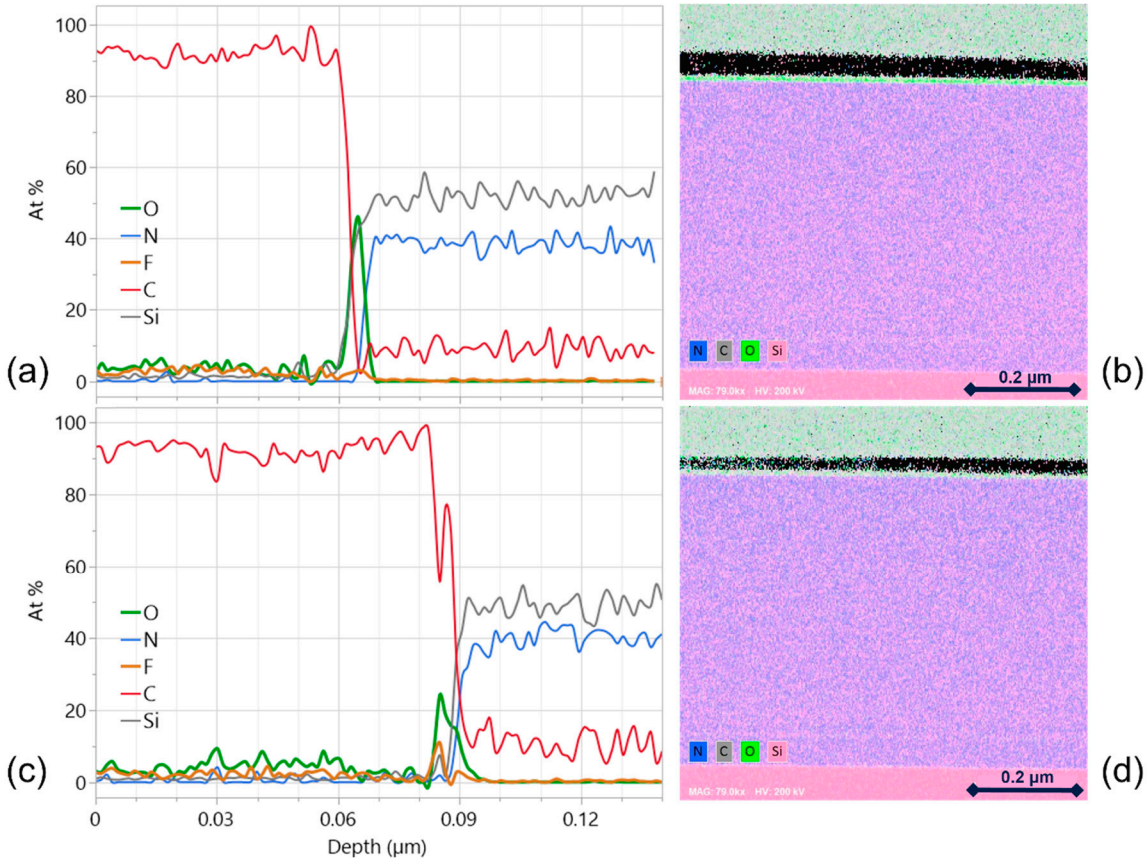

Figure 4. Surface EDX signals of the St_O2 substrate (**a**) and St_CF4 substrate (**c**) with related cross-section TEM image ((**b**) and (**d**), respectively). Formation of an oxidized layer on the substrate interface is deducible by the oxide peak at the interface (revealed by a rapid decrease of C content and increase of Si and N content) and directly visible on the TEM image as a green line for the St_O2 sample, while for the St_CF4 sample, both features are lower in intensity.

Therefore, it can be concluded that O_2 plasma treatment creates an oxidized layer on the SiN substrates, also significantly modifying the surface roughness, while CF_4 plasma induces lower changes, only slightly increasing oxygen content, and leaving roughness unvaried. It is worth noting that the two main variations imposed by the O_2 plasma treatment could be correlated: the newly formed surface layer is most probably composed of SiO_2, which, from the literature, is known for having lower roughness than SiN films [22].

4. Adhesion Analysis

Upon conclusion of the substrate's characterization, the PBO films were deposited, and their adhesion was evaluated by in situ and ex situ nanoindentation under different environmental conditions.

Nanoindentation, as a technique for evaluating the adhesion of a deposited film, can be used in different setups and can provide different outputs depending on the procedure used or on the possible coupling with finite element simulations [9,30]. For example, it is possible to perform cross-section indentations near the interface [31] or axially on the surface of the film under investigation [32]. The latter represents the experimental setup used in this study.

In the case of uniaxial front-view indentation, the tip applies a controlled pressure to the polymer film surface, generating a stress field that extends to the film–substrate interface and induces local delamination events. These events correspond to abrupt changes in the slope of the load-penetration curve, known as "decay event", and enable direct information about the film adhesion through the monitoring of the critical load of delamination. This value, normally stated in μN, in this study has been reported for every sample as the average result of six subsequent indentations and normalized to the maximum applied load, which was kept constant for all tests performed to ensure adequate comparison between the results. For each sample, the six indentations were performed along a line extending 5 mm from the surface of each square sample (of approximately 15 mm per side), ensuring proper extension of the tested surface while excluding the edge areas of the samples, which may undergo unpredictable alterations during environmental control. It is important to note that this approach allows for sensitive detection of interfacial delamination at a certain critical load, but not for the extrapolation of the energy of delamination of the film, a parameter most often used to evaluate the adhesion of a coating. The critical load of delamination permits a qualitative adhesion ranking between the films under comparison, when all the parameters of the test, like the loading rate or the maximum load, are kept uniform across all test replicas.

As a reference, Figure 5 reports the load-penetration curve obtained for the SR_Asd sample tested in ambient conditions (no environmental control). For each individual indentation curve, the load corresponding to the decay event is evaluated, and the average value of these results is considered as the critical delamination load of the examined sample.

Regarding environmental control, the severity of the ambient conditions with varying temperature and relative humidity was considered using an alternative method over those found in the literature. Instead of keeping one of the two values constant while varying the other, in this study, it was decided to vary the two values simultaneously to search for a univocal dependence on the ambient conditions. Therefore, to identify the degree of severity of the environment, it was decided to exploit the dew point, a physical quantity directly dependent on T and RH through the Magnus–Tetens formula:

$$T_{DP} = \frac{b \cdot \alpha(T,RH)}{a - \alpha(T,RH)};\ \alpha(T,RH) = \frac{a \cdot T}{b+T} + \ln\frac{RH}{100}\ ;\ T > 0\ ^\circ\mathrm{C} \begin{cases} a = 17.6 \\ b = 243\ ^\circ C \end{cases} \quad (1)$$

where T_{DP} and T are the dew point and ambient temperature, respectively, (both in °C), RH is the relative humidity, and a and b are two phenomenological constants of the Magnus–Tetens formula.

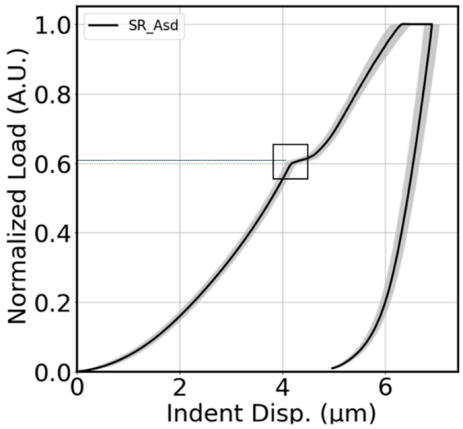

Figure 5. Load-penetration curve obtained by averaging six separated indentations on the SR_Asd sample. The average curve is represented by the marked black line, while the gray band represents the standard deviation. The abrupt change in slope, i.e., the decay event, highlighted in the box, permits evaluation of the critical load of delamination.

The dew point is the temperature at which the air becomes saturated with moisture, causing water vapor to condense into liquid water. It represents the value to which the ambient temperature should drop to bring the relative humidity to reach 100%. Thus, a higher dew point indicates more moisture in the air and a higher absolute humidity.

4.1. Nanoindentation in Ambient Environment

As a first approach, all the samples were tested in ambient conditions before any environmental control to verify the initial PBO adhesion level. Figure 6 reports the average critical load for the different substrates, which is considered a reference for the starting adhesiveness of the analyzed set of samples.

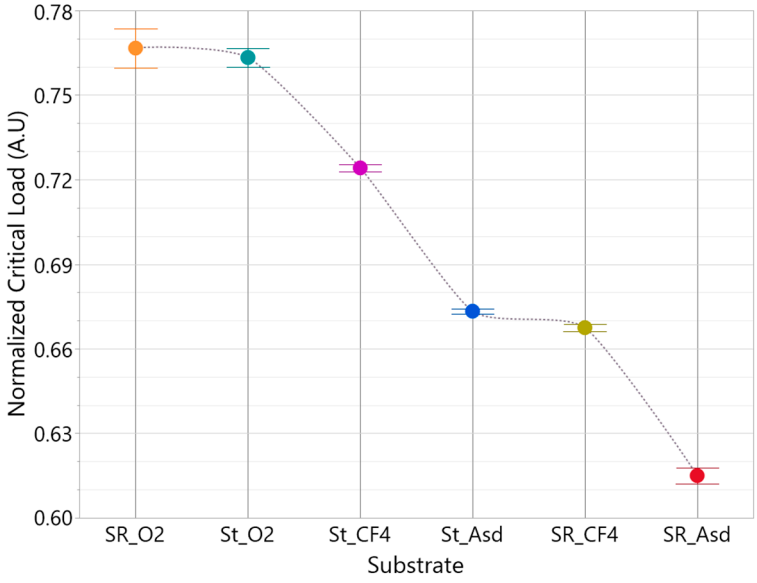

Figure 6. Critical load of the six samples obtained by nanoindentation testing in ambient conditions.

From these first results, it is possible to observe a ranking of the samples, with both plasma treatments increasing PBO adhesion with different intensities, as reported in Table 4. Results related to the as-deposited samples show that a more stoichiometric silicon nitride leads to higher adhesiveness with PBO, as the St_Asd sample reports a critical load 10% higher than the SR_Asd sample. CF_4 plasma leads to an increment of about 8% in the

critical load of both substrate types, independently of the starting stoichiometry, while O_2 plasma increases the value by 13% for the standard substrate and by 24% for the silicon-rich substrate, leading both initial substrates to show the same adhesiveness with PBO. These results further prove the formation of an oxygenated interlayer in the two substrates treated with oxygen, which instead is not formed in the case of the CF_4 plasma.

Table 4. Percentage increment in critical delamination load of as-deposited substrates after plasma treatments.

Initial Substrate	CF_4 Plasma	O_2 Plasma
Standard	8%	13%
Si-rich	8%	24%

Thus the main result of this section states that: (i) increasing silicon content in silicon nitride reduces its adhesiveness regardless of the increase in surface roughness, and (ii) the two plasma treatments operate in a different way, with CF_4 plasma operating a fixed increment of the critical load on both substrates, and the O_2 plasma substantially equalizing the adhesiveness of the two original substrates to an equal and higher value.

4.2. Environmental Control: In Situ Analysis

The analyses conducted in situ with the xSol-Humidity environmental control module provided fundamental information about the adhesive response of the SiN/PBO interface at varying ambient dew points.

As a first result, it is important to note that the load branches of the load-penetration curves do not significantly change their slope as the test environment changes within the evaluated limits, as can be seen in Figure 7. This indicates that the PBO compliance remains nearly constant across tests and that it is therefore reasonable to directly compare the critical delamination loads with each other.

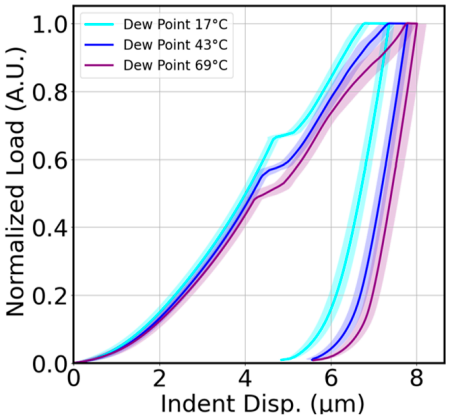

Figure 7. Average load-penetration curve obtained by testing the St_Asd sample in situ at varying ambient dew points. The unvaried slope of the loading branches indicates no major variation in the compliance of the PBO under increasing severity of ambient conditions. The average curve is represented by the marked lines, while the gray bands represent the standard deviations.

Once this point is stated, it is useful to analyze the variation of PBO critical delamination load for increasing severity of the environment in terms of temperature and relative humidity. Figure 8 shows the results for the samples tested at T_{DP} of 43 °C (T = 55 °C and RH = 55%) and T_{DP} of 69 °C (T = 75 °C and RH = 75%) in comparison to the reference values obtained in ambient conditions, which have been considered with a T_{DP} of 10 °C (T = 22 °C and RH = 50%).

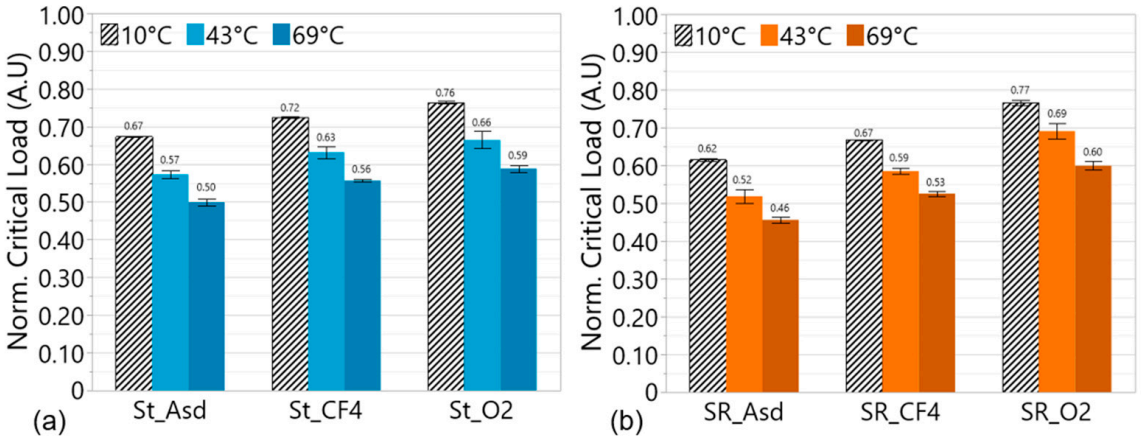

Figure 8. Critical load results for standard SiN samples (**a**) and silicon-rich SiN samples (**b**). While the dashed bar indicates the value obtained under ambient conditions (prior to any environmental control), the colored bars show the results at the middle (43 °C) and high (69 °C) dew points within the tested range.

These results permit identification of three major trends: (I) for a fixed dew point, the substrate ranking observed in the ambient environment remains valid up to the most severe conditions tested in situ, with the SR_O2 sample always showing the higher critical load values (almost identical to St_O2 sample) and the SR_Asd the lower one; (II) all the samples tested in situ in the most severe conditions show a loss of about 25% of their critical load of delamination; (III) the decrease of adhesiveness with increasing dew point is almost constant in all samples, indicating no dependence on substrate selection. This last point indicates that, while plasma treatments increase the absolute adhesiveness of the PBO, they have an insignificant impact on the ambient-related interface deterioration.

Moreover, it is interesting to study the evolution of the critical load with the ambient dew point. Figure 9 reports these trends for plasma-treated samples, which show a sensible decrease in the critical load for low and high dew point ranges and a plateau for mid-range dew points, indicating nonlinear behavior with the environmental conditions.

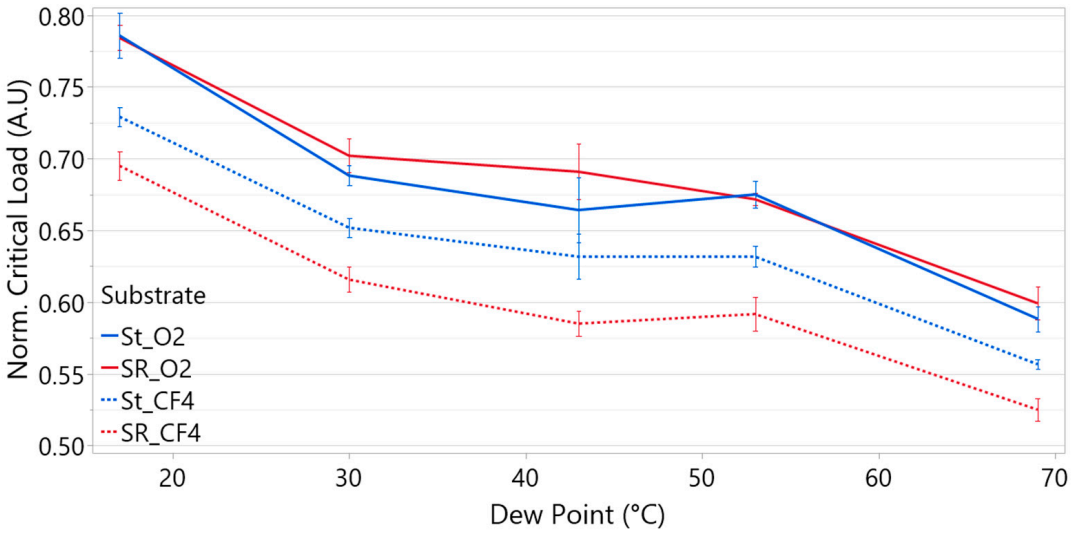

Figure 9. The evolution of the critical load with increasing dew point, tested in situ, is reported for the four plasma-treated samples. In all samples, a similar trend is observed: rapid decline in critical load at low and high dew points and a plateau at mid-range dew points within the investigated range.

4.3. Environmental Control: Ex Situ Analysis

The analysis conducted on samples subjected to the aging process allowed for a direct comparison between ex situ and in situ testing, revealing interesting PBO behavior most probably related to its recovery features.

Figure 10 reports the evolution of the critical load of delamination with ambient dew point for the O_2 plasma-treated samples (i.e., the most resistant to delamination) in the case of the in situ testing and the ex situ testing measured after environmental aging treatments lasting 2 and 7 days. As a reference, the grey band represents the standard deviation of the critical load evaluated in ambient conditions, i.e., 22 °C and 50% RH.

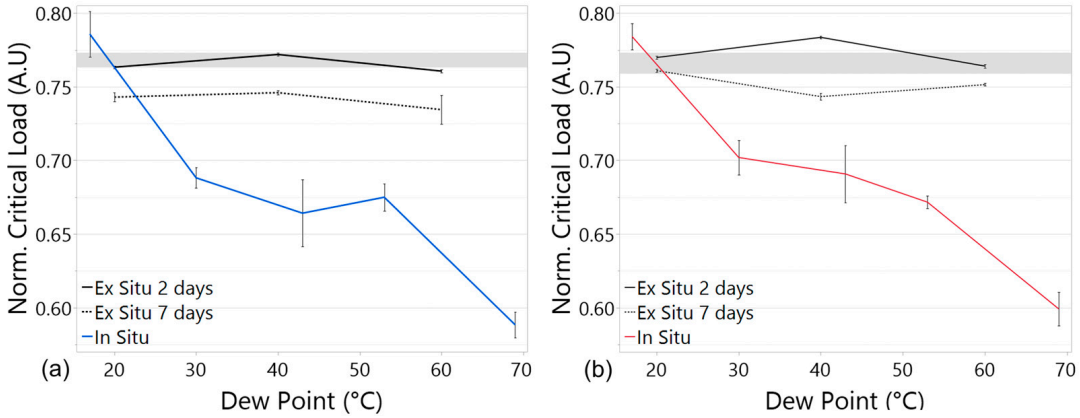

Figure 10. Comparison between the critical load evolution with increasing dew point between in situ and ex situ results for the standard (**a**) and silicon-rich (**b**) SiN samples treated with oxygen plasma. Initial values taken in ambient conditions are reported in gray bands, which represent the standard deviation of the measurements.

The results highlight a clear recovery phenomenon of the PBO's adhesive properties once the samples are removed from the climatic chamber and tested ex situ under laboratory conditions. This effect is particularly evident in samples subjected to 2-day aging, where post-aging critical load values are similar to those measured before aging. Conversely, in samples exposed to more prolonged treatments, i.e., 7 days, a slight reduction of an average 4% in the critical load compared to initial values is observed, which, however, is substantially independent of the environmental condition they were subjected to during aging treatment. A similar behavior has been observed in the as-deposited and CF_4-treated samples and represents a significant difference from the results obtained for in situ tests, where the critical load showed a clear dependence on environment, with a maximum reduction of an average 24% at 69 °C of DP.

5. Discussion

5.1. Substrate Pre-Treatment Effect on Adhesion

On both as-deposited SiN surfaces, PBO adhesion is relatively poor. This is primarily due to the limited surface energy of silicon nitride, which reduces wettability and the potential for strong interfacial bonding. This aspect is caused by the elevated number of silicon-nitrogen (Si-N) or silicon-hydride (Si-H) termination groups present on the SiN surface [3], which do not readily interact chemically with the PBO precursor during curing, resulting in weaker adhesion [33,34]. Between the two as-deposited substrates, PBO shows higher adhesion on the St SiN, probably due to the different roughness and higher chemical stability [3].

Following both O_2 and CF_4 plasma treatments, PBO adhesion has been proven to be improved. However, the mechanisms responsible for this enhancement differ funda-

mentally due to the distinct surface modifications induced by each treatment. To discuss such aspects, it is helpful to observe the monomeric structure of PBO as-spun and after the curing process performed at 350 °C, as shown in Figure 11.

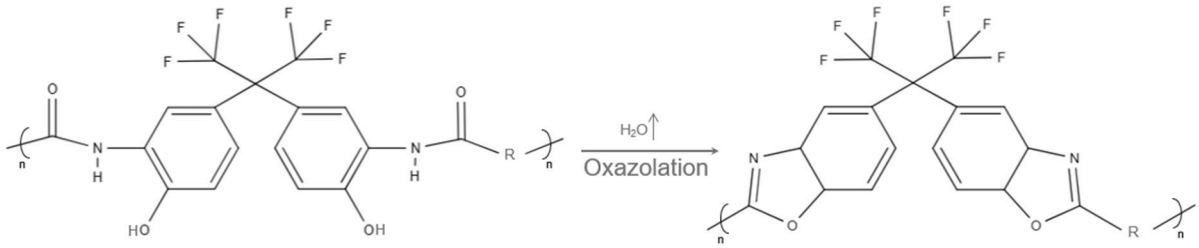

Figure 11. Schematic representation of the analyzed PBO monomer before and after the curing step. As dehydration occurs, the open carbon rings close up, forming oxazole rings through the so-called oxazolation process.

O_2 plasma treatment results in the formation of a thin silicon oxide layer on the SiN surface. This oxide layer is known to be rich in hydrophilic silanol (Si-OH) groups [35]—present in drastically higher amounts with respect to untreated SiN—which are highly reactive with the OH radicals present within the PBO precursor before the curing process. Interactions between these two groups, i.e., silanols and alcohols, are energetically favorable, and they tend to undergo dehydration processes to form covalent bonding through an oxygen atom, producing a water molecule as a byproduct [36]. This condensation mechanism is further enhanced during the curing treatment carried out to initiate oxazolation and is expected on a wide variety of surfaces, constituting the main anchoring and adhesion mechanism of PBO on any substrate, although plasma treatment in O_2 significantly increases its effectiveness. Additionally, the oxide layer increases the surface energy and wettability of the substrate, optimizing spreading and contact area of the PBO film [35]. Overall, these effects significantly strengthen interfacial bonding and thus enhance adhesion. Finally, even if the oxidation effect of the O_2 plasma treatment forms a thicker film on the SR surface with respect to the St one, the PBO adhesion is increased for both substrates and reaches an almost identical value. This indicates that the oxidation of the SiN surface can be a method to increase and standardize its adhesive properties regardless of the deposition parameters used to synthesize it.

It is more complicated to grasp the origins of the adhesion promotion given by the CF_4 plasma treatment. From the experimental results of this work, the treatment does not impact the surface roughness of the substrate (see Table 2). Excluding this aspect, it is plausible to consider that adhesion is promoted by an alteration of the chemical groups present at the interface. Since the adhesion with both substrates is equally increased by 8%, the beneficial effect of the plasma treatment seems to be independent of the SiN stoichiometry. With these considerations, the beneficial effects of CF_4 plasma are associated with surface cleaning of external organic pollutants, which may lead to parasitic bonds with the as-spun PBO [16]. It is hypothesized that such weak bonds could compromise the oxazolation process during curing, leading to the formation of an interlayer between the substrate and the bulk polymer with inferior mechanical performance, which could act as a promoter of crack formation and delamination.

5.2. Moisture Absorption Behavior

The second major finding of this study concerns the role of environmental conditions in the evolution of PBO/SiN adhesion. In situ measurements showed a consistent critical load decrease with increasing ambient T_{DP}, up to a reduction of approximately 25% in the most severe ambient tested, regardless of the substrate analyzed. On the contrary, ex situ

tests exhibit markedly different behavior, with no measurable change in adhesion after 2 days of aging and a small but permanent decrease in critical load (of approximately 4%) after 7 days of aging, without a clear dependence on ambient conditions.

Combined, these results suggest two major points: (i) while the substrate nature significantly affects the initial adhesion, the impact of different environmental conditions is primarily associated with the polymer properties; (ii) ambient-related adhesion degradation is entirely reversible for short exposure time (in situ or 2 days aging) but not after prolonged ones (7 days aging), thus indicating the presence of time-dependent degradation mechanisms with slow kinetic evolution.

This behavior is in line with effects already observed for the hygroscopic swelling of organic compounds [6,13,37]. This is a well-known degradation mechanism observed when polymers absorb moisture under humid conditions—undergoing temporary volumetric expansion and mechanical stress, which could weaken the interface—returning to its initial state following moisture desorption. Shirangi et al. [37] investigated the swelling effects on organic compounds, observing a relationship between the reversibility of the detrimental effects of swelling and dwell time at high moisture content. Considering a diffusion coefficient of water in thin PBO films in the order of 10^{-10} m^2/s [6,12], it is reasonable to consider hygroscopic swelling as fully reversible after 2 days of aging but only partially reversible after 7 days of aging. This would explain the observed critical delamination loads.

While hygroscopic swelling concerns the macro-mechanical behavior of the bulk of the polymeric film, it is also interesting to consider chemical degradation processes at the interface. Interfacial bonding can be weakened by replacing hydrogen bonding, reducing dipole and dispersive interactions, or by breaking chemical bonds through possible hydrolysis reactions [7]. In the system under study, it is plausible that reversible protonation or hydrogen-bonding substitution could explain an immediate, recoverable drop in adhesion observed in situ, while hydrolysis or oxidation reactions, possibly catalyzed by pollutant agents inside the climatic chamber, could be another source of permanent degradation for the samples tested ex situ.

These findings underscore the importance of considering both short-term and long-term environmental effects when evaluating adhesion properties, and highlight the fundamental differences between in situ and ex situ testing of polymeric passivation layers in semiconductor packaging.

6. Conclusions

This study provides a comprehensive assessment of the adhesion performance of PBO films on six different SiN substrates, focusing on the combined influence of O_2 and CF_4 surface plasma treatments and environmental conditions. After characterization of the substrates before PBO deposition, a dual experimental approach was adopted to test PBO adhesion, comparing in situ testing within controlled humidity and temperature environments with ex situ testing following prolonged climatic aging. The key findings are reported below:

- Stoichiometric SiN exhibits about 10% higher initial adhesion to PBO than silicon-rich SiN, despite the latter's higher surface roughness.
- Oxygen plasma treatment improves adhesion by 13% on stoichiometric SiN and by 24% on silicon-rich SiN, attributed to the formation of a reactive silicon oxide layer rich in silanol groups, which equalizes adhesion across substrates.
- CF_4 plasma treatment enhances adhesion by approximately 8% on both substrate types, primarily through surface cleaning rather than oxidation.
- In situ adhesion testing reveals a consistent adhesion loss of up to 25% with increasing environmental dew point (up to 69 °C), underscoring the critical role of moisture in interface degradation.

- Ex situ aging shows that adhesion recovers fully after 2 days of exposure but suffers a small, irreversible reduction of approximately 4% after 7 days, indicating time-dependent degradation mechanisms ascribed to hygroscopic swelling.

In conclusion, this study highlights how the adhesion of a polymer film is influenced by the choice and preparation of the substrate and how its behavior in critical environments can be perceived differently depending on the type of adhesion analysis performed. The results obtained by nanoindentation allowed the identification of substantial differences between in situ and ex situ methods, demonstrating that aging treatments can lead to an overestimation of the film's adhesion due to its fast recovery properties.

In this context, the xSol-Humidity module permits direct probing of the interface while it is immersed in the altered atmosphere, capturing the real temperature and relative humidity of the ambient thanks to proper sensors placed within the small chamber containing the sample, whereas the climatic chamber separates exposure and testing and therefore mainly reveals the small, irreversible modifications that remain after moisture desorption. In situ testing is thus more representative of real operating conditions and well-suited to ranking materials and surface treatments, whereas ex situ aging extends the accessible T–RH range and retention times but tends to underestimate temporary degradation.

Future work could aim at combining and extending both approaches (longer in situ dwells, tailored aging protocols) to gain further insights into the mechanisms behind recoverable and permanent loss of adhesion, or applying the methodology to other organic passivation materials, to rank different materials used as organic passivation in microelectronics in terms of the moisture sensitivity of their adhesion performance. Estimating the energy of adhesion corresponding to the measured critical loads is another relevant future perspective, which would require finite element analysis of the experiment to match experimental observables (e.g., load/displacement curves, extent of delaminated area).

Author Contributions: Conceptualization, S.M. and D.F.; methodology, F.S., E.C. and V.C.; validation, E.C. and V.C.; investigation, F.S.; resources, L.-L.C.; data curation, F.S.; writing—original draft, F.S.; writing—review and editing, F.S., E.C., V.C., S.M., D.F., L.-L.C., A.L.B. and P.Z.; supervision, S.M., D.F., A.L.B. and P.Z.; project administration, A.L.B. and P.Z.; funding acquisition, A.L.B. and P.Z. All authors have read and agreed to the published version of the manuscript.

Funding: Filippo Sabatini acknowledges the Italian Ministry of University and Research (MUR) under the National Recovery and Resilience Plan (PNRR), Mission 4, Component 2, Investment 3.3, as set out in the Ministerial Decree n. 352, for partially funding this research. This research received no other external funding.

Data Availability Statement: Data are available upon request to the corresponding author within the limit of the non-disclosure policy enforced by the company STMicroelectronics.

Acknowledgments: The authors would like to express their gratitude to STMicroelectronics and Politecnico di Milano for their invaluable support and collaboration in this research. This work was carried out as part of a joint effort between the two institutions, combining academic and industrial expertise to achieve the presented results. The authors also acknowledge the contributions of all team members involved in this project. Furthermore, the authors thank Enrica Ravizza and Maurizio Moroni (STMicroelectronics Agrate) for their important contribution in carrying out the XPS and AFM analyses reported in this study, respectively, and all the researchers of the *FMT Physical Laboratory* of STMicroelectronics Agrate for their invaluable support. A special thanks also goes to Manuel Isacchi (STMicroelectronics Agrate) which have offered important support during the preliminary analysis that have then led to this research.

Conflicts of Interest: The authors declare no conflict of interest.

References

1. Zhang, T.; Hu, D.; Jin, J.; Yang, S.; Li, G.; Jiang, J. Introduction of fluorin into PBO polymer chains: Toward higher thermal stability and lower dielectric constant. *Sci. China Ser. E Technol. Sci.* **2009**, *52*, 232–237. [CrossRef]
2. Fukukawa, K.I.; Ueda, M. Recent development of photosensitive polybenzoxazoles. *Polym. J.* **2006**, *38*, 405–418. [CrossRef]
3. Giacomazzi, L.; Umari, P. First-principles investigation of electronic, structural, and vibrational properties of a-Si_3N_4. *Phys. Rev. B-Condens. Matter Mater. Phys.* **2009**, *80*, 144201. [CrossRef]
4. Seiffe, J.; Gautero, L.; Hofmann, M.; Rentsch, J.; Preu, R.; Weber, S.; Eichel, R.A. Surface passivation of crystalline silicon by plasma-enhanced chemical vapor deposition double layers of silicon-rich silicon oxynitride and silicon nitride. *J. Appl. Phys.* **2011**, *109*, 034105. [CrossRef]
5. Song, X.; Gan, B.; Qi, S.; Guo, H.; Tang, C.Y.; Zhou, Y.; Gao, C. Intrinsic nanoscale structure of thin film composite polyamide membranes: Connectivity, defects, and structure–property correlation. *Environ. Sci. Technol.* **2020**, *54*, 3559–3569. [CrossRef]
6. Jain, A.; Gupta, V.; Basu, S.N. A quantitative study of moisture adsorption in polyimide and its effect on the strength of the polyimide/silicon nitride interface. *Acta Mater.* **2005**, *53*, 3147–3153. [CrossRef]
7. Luo, S.; Wong, C.P. Influence of temperature and humidity on adhesion of underfills for flip chip packaging. In *Proceedings of the 2001 51st Electronic Components and Technology Conference (Cat. No. 01CH37220), Orlando, FL, USA, 29 May–1 June 2001*; IEEE: New York, NY, USA, 2001; pp. 155–162.
8. Gupta, V.; Hernandez, R.; Charconnet, P. Effect of humidity and temperature on the tensile strength of polyimide/silicon nitride interface and its implications for electronic device reliability. *Mater. Sci. Eng. A* **2001**, *317*, 249–256. [CrossRef]
9. Naumann, F.; Stephan, T.; Mittag, M.; Klengel, R.; Klengel, S. Analysis of Degradation Effects for Different Epoxy-Based Molding Compounds (EMC) Under High Temperature Aging. In *Proceedings of the 2024 IEEE 10th Electronics System-Integration Technology Conference (ESTC), Berlin, Germany, 11–13 September 2024*; IEEE: New York, NY, USA, 2024; pp. 1–7.
10. Fan, X.; Zhou, J.; Chandra, A. Package structural integrity analysis considering moisture. In *Proceedings of the 2008 58th Electronic Components and Technology Conference, Lake Buena Vista, FL, USA, 27–30 May 2008*; IEEE: New York, NY, USA, 2008; pp. 1054–1066.
11. Jang, C.; Yoon, S.; Han, B. Measurement of the hygroscopic swelling coefficient of thin film polymers used in semiconductor packaging. *IEEE Trans. Compon. Packag. Technol.* **2010**, *33*, 340–346. [CrossRef]
12. He, Y.; Kabiri, M. In-situ characterization of moisture absorption and hygroscopic swelling of an epoxy molding compound for electronic packaging. *J. Therm. Anal. Calorim.* **2022**, *147*, 5667–5675. [CrossRef]
13. He, Y.; Fan, X. In-situ characterization of moisture absorption and desorption in a thin BT core substrate. In *Proceedings of the 2007 Proceedings 57th Electronic Components and Technology Conference, Sparks, NV, USA, 29 May–1 June 2007*; IEEE: New York, NY, USA, 2007; pp. 1375–1383.
14. Zhou, J.; Law, J.S. Effect of non-uniform moisture distribution on the hygroscopic swelling coefficient. *IEEE Trans. Compon. Packag. Technol.* **2008**, *31*, 269–276. [CrossRef]
15. Borcia, C.; Borcia, G.; Dumitrascu, N. Surface treatment of polymers by plasma and UV radiation. *Rom. J. Phys.* **2011**, *56*, 224–232.
16. Gaddam, S.; Kazi, H.; Dong, B.; Driver, M.; Kelber, J. Surface cleaning for enhanced adhesion to packaging surfaces: Effect of oxygen and ammonia plasma. *J. Vac. Sci. Technol. A* **2015**, *33*, 021301. [CrossRef]
17. An, R.; Huang, L.; Mineart, K.P.; Dong, Y.; Spontak, R.J.; Gubbins, K.E. Adhesion and friction in polymer films on solid substrates: Conformal sites analysis and corresponding surface measurements. *Soft Matter* **2017**, *13*, 3492–3505. [CrossRef] [PubMed]
18. Wu, G.M.; Hung, C.H.; You, J.H.; Liu, S.J. Surface modification of reinforcement fibers for composites by acid treatments. *J. Polym. Res.* **2004**, *11*, 31–36. [CrossRef]
19. Hang, T.; Ling, H.; Xiu, Z.; Li, M.; Mao, D. Study on the adhesion between epoxy molding compound and nanocone-arrayed Pd preplated leadframes. *J. Electron. Mater.* **2007**, *36*, 1594–1598. [CrossRef]
20. Cho, Y.; Kim, G.; Cho, Y.; Lee, S.Y.; Minsky, H.; Turner, K.T.; Gianola, D.S.; Yang, S. Orthogonal control of stability and tunable dry adhesion by tailoring the shape of tapered nanopillar arrays. *Adv. Mater.* **2015**, *27*, 7788–7793. [CrossRef] [PubMed]
21. Lu, C.H.; Kho, Y.T.; Yang, Y.T.; Chen, Y.P.; Chen, C.P.; Hung, T.T.; Chen, C.-F.; Chen, K.N. Adhesion property of polyimide and passivation layer for polymer/metal wafer-level hybrid bonding in 3D integration. In *Proceedings of the 2018 IEEE 68th Electronic Components and Technology Conference (ECTC), San Diego, CA, USA, 29 May–1 June 2018*; IEEE: New York, NY, USA, 2018; pp. 401–406.
22. Grady, M.E.; Geubelle, P.H.; Sottos, N.R. Interfacial adhesion of photodefinable polyimide films on passivated silicon. *Thin Solid Film.* **2014**, *552*, 116–123. [CrossRef]
23. Silbernagl, D.; Sturm, H.; Cappella, B. Influence of Film− Substrate Adhesion on the Mechanical Properties of Thin Polymer Films. *Langmuir* **2009**, *25*, 5091–5097. [CrossRef] [PubMed]
24. Staszel, C.; Sinha-Ray, S.; Yarin, A.L.; Pourdeyhimi, B. Adhesion of blended polymer films. *Polymer* **2017**, *112*, 92–101. [CrossRef]
25. Hohlfelder, R.J.; Maidenberg, D.A.; Dauskardt, R.H.; Wei, Y.; Hutchinson, W. Adhesion of benzocyclobutene-passivated silicon in epoxy layered structures. *J. Mater. Res.* **2001**, *16*, 243–255. [CrossRef]

26. Tsurumi, N.; Tsuji, Y.; Masago, N.; Yoshizawa, K. Elucidation of adhesive interaction between the epoxy molding compound and Cu lead frames. *ACS Omega* **2021**, *6*, 34173–34184. [CrossRef]
27. Liu, D.; Chen, P.; Chen, M.; Liu, Z. Improved interfacial adhesion in PBO fiber/bismaleimide composite with oxygen plasma plus aging and humid resistance properties. *Mater. Sci. Eng. A* **2012**, *532*, 78–83. [CrossRef]
28. Cattarinuzzi, E.; Gastaldi, D.; Vena, P.; Pozzobon, F.; Guarino, L.; Cecchetto, L.; Andreini, A. Identification of traction-separation parameters by means of peel testing and in situ confocal microscopy. *J. Micromech. Microeng.* **2019**, *29*, 034001. [CrossRef]
29. Brucker Corporation. In Operando Nanomechanics. 2025. Available online: https://www.bruker.com/en/products-and-solutions/test-and-measurement/nanomechanical-test-systems/nanomechanical-test-system-upgrade-options/in-operando-nanomechanics (accessed on 15 July 2025).
30. Konnerth, J.; Jäger, A.; Eberhardsteiner, J.; Müller, U.; Gindl, W. Elastic properties of adhesive polymers. II. Polymer films and bond lines by means of nanoindentation. *J. Appl. Polym. Sci.* **2006**, *102*, 1234–1239. [CrossRef]
31. Hartleb, M.; Imrich, P.; Zechner, J.; Walter, T.; Petersmann, M.; Khatibi, G. Adhesion properties of polyimide coated stacks: An in-depth analysis of the cross-sectional nanoindentation method. *Heliyon* **2024**, *10*, e40967. [CrossRef] [PubMed]
32. Kleinbichler, A.; Pfeifenberger, M.J.; Zechner, J.; Moody, N.R.; Bahr, D.F.; Cordill, M.J. New insights into nanoindentation-based adhesion testing. *JOM* **2017**, *69*, 2237–2245. [CrossRef]
33. Schall, J.D.; Morrow, B.H.; Carpick, R.W.; Harrison, J.A. Effects of–H and–OH Termination on Adhesion of Si–Si Contacts Examined Using Molecular Dynamics and Density Functional Theory. *Langmuir* **2024**, *40*, 4601–4614. [CrossRef] [PubMed]
34. Brunet, M.; Aureau, D.; Chantraine, P.; Guillemot, F.; Etcheberry, A.; Gouget-Laemmel, A.C.; Ozanam, F. Etching and chemical control of the silicon nitride surface. *ACS Appl. Mater. Interfaces* **2017**, *9*, 3075–3084. [CrossRef] [PubMed]
35. Liu, L.H.; Michalak, D.J.; Chopra, T.P.; Pujari, S.P.; Cabrera, W.; Dick, D.; Veyan, J.-F.; Hourani, R.; Halls, M.D.; Zuilhof, H.; et al. Surface etching, chemical modification and characterization of silicon nitride and silicon oxide—Selective functionalization of Si_3N_4 and SiO_2. *J. Phys. Condens. Matter* **2016**, *28*, 094014. [CrossRef] [PubMed]
36. Yamamoto, S.; Kuwahara, R.; Tanaka, K. Effects of chemistry of silicon surfaces on the curing process and adhesive strength for epoxy resin. *ACS Appl. Polym. Mater.* **2022**, *4*, 6038–6046. [CrossRef]
37. Shirangi, M.H.; Michel, B. Mechanism of moisture diffusion, hygroscopic swelling, and adhesion degradation in epoxy molding compounds. In *Moisture Sensitivity of Plastic Packages of IC Devices*; Springer: Boston, MA, USA, 2010; pp. 29–69.